Methods

A test of the 'one-point method' for estimating maximum carboxylation capacity from field-measured, light-saturated photosynthesis

Martin G. De Kauwe[1], Yan-Shih Lin[1], Ian J. Wright[1], Belinda E. Medlyn[2], Kristine Y. Crous[2,3], David S. Ellsworth[2], Vincent Maire[4], I. Colin Prentice[1,5], Owen K. Atkin[6], Alistair Rogers[7], Ülo Niinemets[8,9], Shawn P. Serbin[7], Patrick Meir[10,11], Johan Uddling[12], Henrique F. Togashi[1,13], Lasse Tarvainen[14], Lasantha K. Weerasinghe[6,15], Bradley J. Evans[13,16], F. Yoko Ishida[17] and Tomas F. Domingues[18]

[1]Department of Biological Sciences, Macquarie University, Sydney, NSW 2109, Australia; [2]Hawkesbury Institute for the Environment, Western Sydney University, Locked Bag 1797, Penrith, NSW 2751, Australia; [3]Birmingham Institute of Forest Research, University of Birmingham, Edgbaston, B15 2TT, UK; [4]Université du Québec à Trois-Rivières, Trois-Rivières, QC G9A 5H7, Canada; [5]AXA Chair of Biosphere and Climate Impacts, Grand Challenges in Ecosystems and the Environment and Grantham Institute – Climate Change and the Environment, Department of Life Sciences, Imperial College London, Silwood Park Campus, Buckhurst Road, Ascot, SL5 7PY, UK; [6]ARC Centre of Excellence in Plant Energy Biology, Research School of Biology, The Australian National University, Building 134, Canberra, ACT 2601, Australia; [7]Biological, Environmental and Climate Sciences Department, Brookhaven National Laboratory, Upton, NY 11973, USA; [8]Institute of Agricultural and Environmental Sciences, Estonian University of Life Sciences, Kreutzwaldi 1, Tartu 51014, Estonia; [9]Estonian Academy of Sciences, Kohtu 6, 10130 Tallinn, Estonia; [10]Research School of Biology, The Australian National University, Canberra, ACT 0200, Australia; [11]School of Geosciences, University of Edinburgh, Edinburgh, EH9 3JN, UK; [12]Department of Biological and Environmental Sciences, University of Gothenburg, PO Box 461, SE-40530, Gothenburg, Sweden; [13]Terrestrial Ecosystem Research Network, Ecosystem Modelling and Scaling Infrastructure, The University of Sydney, Sydney, NSW 2006, Australia; [14]Department of Forest Ecology and Management, Swedish University of Agricultural Sciences (SLU), SE-901 83, Umeå, Sweden; [15]Faculty of Agriculture, University of Peradeniya, Peradeniya 20400, Sri Lanka; [16]Department of Environmental Sciences, The University of Sydney, Sydney, NSW 2006, Australia; [17]College of Marine and Environmental Sciences, Centre for Tropical Environmental and Sustainability Science, James Cook University, Cairns, Qld 4870, Australia; [18]Faculdade de Filosofia Ciências e Letras de Ribeirão Preto, Universidade de São Paulo, Av Bandeirantes, 3900, CEP 14040-901, Bairro Monte Alegre, Ribeirão Preto, São Paulo, Brazil

Author for correspondence:
Martin G. De Kauwe
Tel: +61 2 9850 9256
Email: mdekauwe@gmail.com

Summary

- Simulations of photosynthesis by terrestrial biosphere models typically need a specification of the maximum carboxylation rate (V_{cmax}). Estimating this parameter using A–C_i curves (net photosynthesis, A, vs intercellular CO_2 concentration, C_i) is laborious, which limits availability of V_{cmax} data. However, many multispecies field datasets include net photosynthetic rate at saturating irradiance and at ambient atmospheric CO_2 concentration (A_{sat}) measurements, from which V_{cmax} can be extracted using a 'one-point method'.
- We used a global dataset of A–C_i curves (564 species from 46 field sites, covering a range of plant functional types) to test the validity of an alternative approach to estimate V_{cmax} from A_{sat} via this 'one-point method'.
- If leaf respiration during the day (R_{day}) is known exactly, V_{cmax} can be estimated with an r^2 value of 0.98 and a root-mean-squared error (RMSE) of 8.19 $\mu mol\ m^{-2}\ s^{-1}$. However, R_{day} typically must be estimated. Estimating R_{day} as 1.5% of V_{cmax}, we found that V_{cmax} could be estimated with an r^2 of 0.95 and an RMSE of 17.1 $\mu mol\ m^{-2}\ s^{-1}$.
- The one-point method provides a robust means to expand current databases of field-measured V_{cmax}, giving new potential to improve vegetation models and quantify the environmental drivers of V_{cmax} variation.

Introduction

Photosynthesis is a primary driver of the terrestrial carbon cycle (Prentice *et al.*, 2001; Beer *et al.*, 2010) and accurate modelling of this process is critical for projecting the response of the terrestrial biosphere to environmental change (Friedlingstein *et al.*, 2014). Terrestrial biosphere models (TBMs, including ecosystem, land surface and vegetation models) almost universally

simulate photosynthesis following the leaf biochemical model of Farquhar *et al.* (1980), or a variant of this approach (Collatz *et al.*, 1991). This approach relies on the accurate estimation of two key model parameters: V_{cmax}, the maximum carboxylation rate, and J_{max}, the maximum rate of electron transport (von Caemmerer, 2000). A third term, triose-phosphate utilization, is often ignored as it is thought to seldom limit photosynthesis under field conditions (Sharkey, 1985; but see Ellsworth *et al.*, 2015). In many cases, both V_{cmax} and J_{max} scale linearly with leaf nitrogen (N) (Field & Mooney, 1986; Hirose & Werger, 1987), although the scaling with N can differ among biomes (Meir *et al.*, 2002; Domingues *et al.*, 2015). V_{cmax} and J_{max} also tend to be closely correlated, a fact that some models exploit by assuming J_{max} can be determined through a fixed relationship with V_{cmax} (see Niinemets & Tenhunen, 1997; for a critique), or, at least, assuming that variation in the two properties is tightly coordinated (Chen *et al.*, 1993; Maire *et al.*, 2012). Nevertheless, V_{cmax} and J_{max} both vary considerably (up to 30-fold) among species (Walker *et al.*, 2014; Ali *et al.*, 2015a,b), among and within plant functional types (PFTs) (Wullschleger, 1993; Kattge *et al.*, 2009; Maire *et al.*, 2012; Ali *et al.*, 2015a,b), and within individual species. Given this large variability, it is perhaps unsurprising that TBMs have demonstrated considerable sensitivity in simulated carbon fluxes owing to uncertainty in these parameters (Bonan *et al.*, 2011; Piao *et al.*, 2013). As a consequence, these parameters are often used as a method of model 'tuning' to obtain more accurate fluxes (which we consider as obtaining the 'right answer for the wrong reasons'), rather than as a means of characterizing a PFT-specific trait (Rogers, 2014).

Traditionally, the photosynthesis model parameters V_{cmax} and J_{max} have been estimated by fitting the Farquhar *et al.* (1980) photosynthesis model directly to photosynthetic CO_2 response curves, where photosynthesis is measured at several CO_2 concentrations and under saturating irradiance (net photosynthesis, A (μmol m^{-2} s^{-1}), vs intercellular CO_2 concentration, C_i (μmol mol^{-1}) – so-called A–C_i curves). However, accurately determining these parameters from such measurements is not a straightforward process (see Long & Bernacchi, 2003). First, A–C_i data are time-consuming to collect: each CO_2 response curve may take 1 h to set up and measure, particularly in stressed plants where stomatal closure may even prohibit such measurements. Second, a number of competing methods exist for fitting the data (Dubois *et al.*, 2007; Sharkey *et al.*, 2007; Patrick *et al.*, 2009; Gu *et al.*, 2010; Feng & Dietze, 2013) and, depending on the chosen method, parameter estimates may vary even for the same datasets (Miao *et al.*, 2009; Niinemets *et al.*, 2009). Many individual experimental studies tend to focus on only a small number of species and, more often than not, they concern plants grown and measured in controlled environments (laboratory or glasshouse). As a result, compared with many plant traits, there is a general paucity of field-measured V_{cmax} and J_{max} data, which probably undermines the accuracy of model simulations of terrestrial photosynthesis. The largest data compilations to date included V_{cmax} data based on A–C_i curve analysis for 127 species (Ali *et al.*, 2015a,b), 114 species (Walker *et al.*, 2014), 130 species (Sun *et al.*, 2014) and 109 species (Wullschleger, 1993), but it is

unclear what proportion of these data were for field-grown plants, or what total species number these represent, with many individual datasets appearing in more than one compilation. Currently in the TRY database (http://www.try-db.org; accessed 7 July 2015) there are georeferenced V_{cmax} data for 353 species (of which *c.* 250 were obtained from A–C_i curves).

In contrast to the relatively limited number of field-measured A–C_i curves, there is a plethora of net photosynthesis measurements obtained in the field at ambient [CO_2] and at saturating irradiance (A_{sat}) – for example, 1500 species were included in the compilation by Maire *et al.* (2015; dataset assembled in 2008), the TRY database currently contains georeferenced photosynthesis data for 2192 species (8522 individual observations), and in recent years there have been a number of large field campaigns, from which the data are yet to make it into these types of databases. Together, these A_{sat} data represent species from large parts of the globe, and all PFTs (Kattge *et al.*, 2011), but are currently left out of analyses of V_{cmax}. By virtue of their global coverage, analyses of A_{sat} have included quantification of latitudinal, climate- and soil-related trends, including modulation of relationships between A_{sat} and other leaf traits (Reich *et al.*, 1997; Reich *et al.* 2009; Wright *et al.*, 2005; Ordonez & Olff, 2013; Maire *et al.*, 2015). When corresponding values of C_i and leaf temperature are reported with each A_{sat} measurement, and if one assumes that photosynthesis at saturating irradiance is Rubisco-limited (rather than being limited by ribulose 1,5-bisphosphate (RuBP) regeneration), and that the value of leaf mitochondrial respiration in the light (i.e. 'day' respiration, R_{day}) can be estimated, then the V_{cmax} value required to support the observed rate of A_{sat} can be estimated. This estimated quantity is hereafter referred to as $\hat{V}_{cmax}$, and the method as the 'one-point method' (Wilson *et al.*, 2000). However, whether A_{sat}-dependent estimates of $\hat{V}_{cmax}$ are an accurate reflection of the V_{cmax} values obtained from full A–C_i curves remains uncertain. In the absence of measurements of C_i, values may be estimated from data reported for stomatal conductance and ambient [CO_2]. Values for R_{day} may be estimated either from a relationship with dark respiration, R_{dark}, or by assuming a relationship with V_{cmax} (see later).

Although several studies have indeed done this – used measurements of A_{sat} and associated parameters to estimate $\hat{V}_{cmax}$ (Niinemets, 1999; Wilson *et al.*, 2000; Kosugi *et al.*, 2003; Grassi *et al.*, 2005; Kattge *et al.*, 2009; Uddling *et al.*, 2009; Niinemets *et al.*, 2015) – a thorough examination of the issues associated with this approach has not been made. That said, preliminary tests of the approach were encouraging. For five tree and five understorey species, Wilson *et al.* (2000) estimated V_{cmax} from A–C_i curves as well as from independent measurements of the assimilation rate, C_i at the ambient external CO_2 concentration (360 μmol mol^{-1}) and a constant value of R_{day} (*c.* 0.5 μmol m^{-2} s^{-1}). The two sets of estimates were tightly correlated ($r^2 = 0.97$) with an intercept not statistically different from zero, but with a small bias in the slope (1.08). Grassi *et al.* (2005) demonstrated that this method could be used to accurately estimate V_{cmax} for three deciduous forest species ($r^2 = 0.97$; slope = 0.96). Given the global coverage of A_{sat} data, there could be great potential for deriving $\hat{V}_{cmax}$ from datasets such as that of

Maire *et al.* (2015), or the TRY database (Kattge *et al.*, 2011), providing a means to dramatically expand the species and geographic coverage of V_{cmax} estimates from field-grown plants in global databases. Nevertheless, employing this approach may result in errors and/or bias, which leads to the question and the focus of this study: how robust is the so-called one-point method for estimating V_{cmax}? Errors in estimation are principally likely to occur if the biochemical limitation to A_{sat} is not Rubisco activity, or if the estimate of R_{day} is biased (Fig. 1).

We tested how well the one-point method works, by estimating V_{cmax} from complete A–C_i response curves and comparing these values with V_{cmax} estimated using the one-point method applied to the A_{sat} data extracted from these curves. To this end, we compiled 1394 A–C_i response curves, from 564 species. These data represent by far the largest compilation of field-measured photosynthetic CO_2 response data to date. These data are taken from all vegetated continents – from the Arctic to the tropics – and so represent a broad spread of site climates (Supporting Information Fig. S1). Using this dataset, we sought to test the following hypotheses. The first, hypothesis 1, is that under ambient CO_2 and saturating irradiance, A_{sat} is normally Rubisco-limited, or colimited by Rubisco and electron transport (a requirement for the one-point method to be valid). There are environmental conditions where this is less likely to be true, leading to the following additional sub-hypotheses: (1a) in mesophytic leaves growing in wet and/or humid environments, the effective operational C_i for leaves is likely to be high, meaning the leaf is more likely to be electron transport-limited, and thus V_{cmax} values are more likely to be underestimated; and (1b) the $J_{max} : V_{cmax}$ ratio at 25°C has been found to decline with increasing growth temperature (Dreyer *et al.*, 2001; Medlyn *et al.*, 2002b; Kattge & Knorr, 2007; Lin *et al.*, 2013). As a result, the leaf is more likely to be electron transport-limited at higher growth temperatures; thus we also hypothesize an underestimation of V_{cmax} at higher growth temperatures. Hypothesis 2 states that estimates of V_{cmax} would in general be less accurate for leaves operating at low A_{sat} and/or low g_s because the cumulative effect of errors in the various underlying assumptions would contribute to a lower signal-to-noise ratio. And hypothesis 3 suggests that uncertainties in R_{day} can contribute to greater bias for estimating V_{cmax} using the one-point method.

In this study we provide a thorough analysis of the one-point method for estimating carboxylation capacity from point measurements of light-saturated photosynthesis, and indicate the conditions under which it works best or may be subject to greater errors. Our primary purpose is to find out whether it would be viable to markedly expand plant trait databases of maximum carboxylation capacity, V_{cmax}, by supplementing those data acquired from A–C_i curves with values derived from A_{sat} by the one-point method.

Materials and Methods

Datasets

We collated 1394 A–C_i curve measurements of upper canopy leaves from 564 C3 species (91 families) and 46 field sites across various ecosystems, including Arctic tundra, boreal and temperate forest, semiarid woodlands and tropical forest (Table 1; Fig. S1). In most cases, measurements were made using the LI-6400 portable photosynthesis system (Li-Cor Inc., Lincoln, NE, USA), except for one dataset obtained in Estonia which was measured using a customized open system (Niinemets, 1998). We selected data where measurements were first conducted at ambient CO_2 concentration (360–400 µmol mol^{-1}, depending on the year of collection) and saturating irradiance conditions (photosynthetic photon flux density (PPFD) between 1000 and 2000 µmol m^{-2} s^{-1}). The measurements then progressed through a series of stepwise changes in CO_2 concentration spanning subambient (40–400 µmol mol^{-1}) and superambient saturating CO_2 concentration (typically > 700 µmol mol^{-1}). During each A–C_i response curve measurement, leaf temperatures were maintained close to the site ambient temperature, ranging from 6 to 40°C. Any measurements obtained that did not follow this protocol, for example in cases where the first measurement was recorded at subambient CO_2, were not used in our analyses.

The data from this project will be made available once the remaining individual source datasets have been published as part of primary empirical papers. Data availability will be summarized and updated as appropriate at https://wrightlab.wordpress.com/datasets/.

Estimation of apparent V_{cmax}, J_{max} and R_{day} from A–C_i response curves

We first estimated apparent V_{cmax}, J_{max} and R_{day} by fitting each field-measured A–C_i curve using the C3 photosynthesis model of Farquhar *et al.* (1980). Several different estimates for the temperature dependence of K_c, the Michaelis constant for CO_2
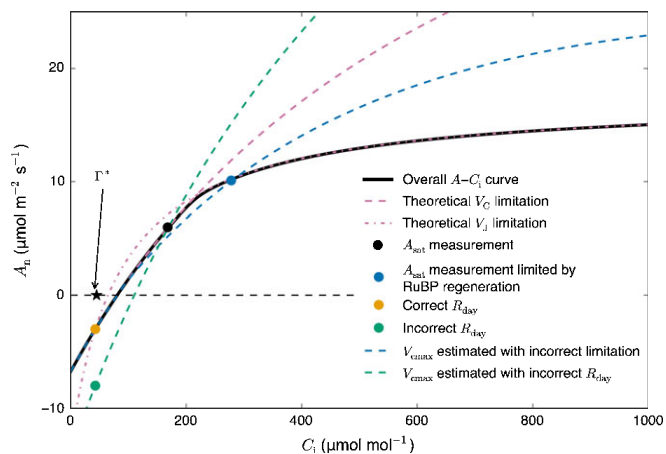

Fig. 1 Conceptual figure demonstrating how errors could arise when using the one-point method to estimate the maximum carboxylation rate (V_{cmax}). When day respiration (R_{day}) is correct (dark yellow point) and net photosynthetic rate at saturating irradiance (A_{sat}) is Rubisco-limited (black point), V_{cmax} is correctly estimated (dashed purple line). When A_{sat} is ribulose 1,5-bisphosphate regeneration (RuBP)-limited (blue point), V_{cmax} will be underestimated (dashed blue line). If R_{day} is overestimated (green point), V_{cmax} will be overestimated (dashed green line). C_i, intercellular CO_2 concentration; A_n, net photosynthesis.

Table 1 List of the datasets, site locations, vegetation types and associated references used in this study

Dataset	Site	Longitude	Latitude	References	Vegetation type
Ellsworth/Crous (51 species)	Aspen FACE, WI, USA	45.68	−89.63	Ellsworth *et al.* (2004)	Temperate broadleaf deciduous forest
	Blue Mountains, NSW, Australia	−33.71	150.55	Ellsworth *et al.* (2015)	Open eucalypt forest
	Cape Tribulation crane site, QLD, Australia	−16.10	145.45	Unpublished	Lowland tropical rainforest
	Carolina Beach, NC, USA	34.05	−77.91	Unpublished	Temperate evergreen forest
	Carolina Lake, NC, USA	35.90	−79.09	Ellsworth *et al.* (2004)	Temperate needle-leaved deciduous forest
	Cedar Creek, Long Term Ecological Research, USA	45.41	−93.19	Crous *et al.* (2010)	Temperate savanna
	Cocoparra National Park, NSW, Australia	−34.17	146.23	Unpublished	*Callitris* pine woodland
	Driftway Cumberland Plain, Richmond, NSW, Australia	−33.62	150.74	Ellsworth *et al.* (2015)	Open eucalypt forest
	Duke Forest, NC, USA	35.97	−79.10	Ellsworth *et al.* (2004, 2012)	Temperate evergreen forest
	Endla bog, Endla, ESTONIA	58.86	26.17	Niinemets *et al.* (2001)	Boreal evergreen bog
	Hawkesbury, Richmond, NSW, Australia	−33.61	150.74	Crous *et al.* (2013); Ellsworth *et al.* (2015)	Open eucalypt forest
	Illawarra, Robertson, NSW, Australia	−34.62	150.71	Ellsworth *et al.* (2015)	Wet sclerophyll forest
	Kuring-Gai National Park (Murrua Track), NSW, Australia	−33.69	151.14	Unpublished	Open eucalypt forest
	La Sueur National Park, WA, Australia	−30.19	115.14	Ellsworth *et al.* (2015)	Kwongan woodland
	Nevada Test Site, NV, USA	36.77	−115.97	Ellsworth *et al.* (2004)	Mojave desert
	Saginaw forest, MI, USA	42.27	−83.81	Unpublished	Temperate broadleaf deciduous forest
	UMBS Pellston, MI, USA	45.56	−84.72	Unpublished	Temperate broadleaf deciduous forest
	Mill Haft, Staffordshire, UK	52.80	2.30	Unpublished	Temperate broadleaf deciduous forest
JACARE (366 species)	Allpahuayo, Loreto, Peru (*c.* 100 m above sea level)	−3.95	−73.44	Atkin *et al.* (2015); Y. Malhi (unpublished)	Humid Amazonian lowland forest
	Cuzco Amazonico, Peru	−3.37	−72.97	Malhi *et al.* (2014); Anderson *et al.* (2009)	Forests over alluvial terrain
	Esperanza, Peru	−2.48	−71.97	Girardin *et al.* (2014a,b)	Upper limit of the cloud forest
	Jenaro Herrera, Peru	−4.88	−73.63	del Aguila-Pasquel *et al.* (2014)	Humid Amazonian lowland forest
	San Pedro, Peru	−6.54	−77.71	Huasco *et al.* (2014)	Cloud forest
	Sucusari, Peru	−3.25	−72.91	Atkin *et al.* (2015)	Humid Amazonian lowland forest
	Tambopata, Peru	−13.02	−69.60	Huasco *et al.* (2014)	Humid Amazonian lowland forest
	Trocha Union, Peru	−13.03	−71.49	Huasco *et al.* (2014)	Montane cloud forest
	Wayquecha, Peru	−13.12	−71.58	Girardin *et al.* (2014a,b)	Upper limit of the cloud forest
Togashi (51 species)	Great Western Woodland, WA, Australia	−30.25	−30.25	H. Togashi (unpublished)	Temperate eucalyptus woodland
	Robson Creek, QLD, Australia	−17.25	145.75	H. Togashi (unpublished)	Tropical rainforest
TROBIT (44 species)	Asukese, Ghana	7.14	−2.45	Domingues *et al.* (2010)	Humid tropical lowland forest
	Bissiga, Burkina Faso	12.73	−1.16	Domingues *et al.* (2010)	Tropical woody savanna
	Bissiga, Burkina Faso	12.73	−1.17	Domingues *et al.* (2010)	Tropical woody savanna
	Boabeng-Fiema, Ghana	7.71	−1.69	Domingues *et al.* (2010)	Seasonal tropical forest
	Dano, Burkina Faso	10.94	−3.15	Domingues *et al.* (2010)	Open tropical savanna
	Hombori, Mali	15.34	−1.47	Domingues *et al.* (2010)	Dry grass savanna
	Kogyae, Ghana	7.30	−1.18	Domingues *et al.* (2010)	Tropical woody savanna
Serbin (21 species)	Coachella Valley Agricultural Research Station, CA, USA	33.52	−116.16	Serbin *et al.* (2015)	Vineyard and date palm
	Loma Ridge Coastal Sagescrub EC site, CA, USA	33.73	−117.70	S. Serbin (unpublished)	Coastal sage-scrub
	Sierra Mixed Conifer EC site, CA, USA	37.07	−119.20	S. Serbin (unpublished)	Mixed conifer/broadleaf forest
	San Joaquin Experimental Range, CA, USA	37.08	−119.73	S. Serbin (unpublished)	Semiarid woodland
	San Jacinto James Reserve EC tower site, CA, USA	33.81	−116.77	S. Serbin (unpublished)	Mixed conifer/broadleaf forest
	UW-Madison Arboretum, WI, USA	43.04	−89.43	S. Serbin (unpublished)	Temperate broadleaf deciduous forest

Table 1 (Continued)

Dataset	Site	Longitude	Latitude	References	Vegetation type
Domingues (24 species)	Tapajós, Brazil	−3.75	−56.25	Domingues et al. (2005)	Humid Amazonian lowland forest
Niinemets (three species)	Ülenurme, Estonia	58.30	26.70	Niinemets (1998)	Temperate broadleaf deciduous forest
Rogers (seven species)	Barrow Environmental Observatory, Barrow, AK, USA	71.32	156.62	A. Rogers (unpublished)	Tundra
Tarvainen (one species)	Skogaryd, Sweden	58.23	12.09	Tarvainen et al. (2013)	Hemiboreal coniferous forest

(μmol mol^{-1}), K_o, the Michaelis constant for O_2 (mmol mol^{-1}), and Γ^*, the CO_2 compensation point in the absence of mitochondrial respiration (μmol mol^{-1}), can be found in the literature (Badger & Collatz, 1977; Jordan & Ogren, 1984; Brooks & Farquhar, 1985; Bernacchi et al., 2001; Crous et al., 2013). We chiefly use values taken from Bernacchi et al. (2001), hereafter denoted B01, in common with many TBMs. To test whether the choice of values for these parameters affects the success of the one-point method, we also used two alternative sets of these parameters, namely those advanced by Badger & Collatz (1977) (hereafter denoted BC77) and Crous et al. (2013) (hereafter denoted C13): see Table 2 for details. The Γ^* temperature dependencies of tobacco (B01) and eucalypt (C13) represent two extremes of the most and least temperature-sensitive Γ^* responses, respectively, using in vivo gas exchange methods (K. Crous, unpublished). To contrast with in vitro methods, we also considered the temperature response of Γ^* in *Atriplex glabriuscula* (BC77).

The intercellular concentration of oxygen (O_i) was assumed to be 210 mmol mol^{-1} for all data collected at sea level. In other datasets, O_i, C_i, and Γ^* were corrected for the effect of elevation on partial pressure by multiplying by the observed pressure readings and correcting units to μbar, mbar and mbar, respectively. For calculations with the B01 and C13 temperature dependencies, K_o and K_c were converted to units of μbar and mbar, respectively. This was done by assuming that the original measurements were obtained at an average atmospheric pressure of 987 mbar in Urbana, IL (von Caemmerer et al., 2009). K_o and K_c values from BC77 were simply converted from concentration to partial pressures assuming a standard pressure of 1011.35 mbar.

We assumed an infinite mesophyll conductance (g_m); therefore the estimated V_{cmax} and J_{max} values should be regarded as apparent values (Evans, 1986; Sun et al., 2014), as generally used in TBMs and reported in most of the ecophysiological literature. A closer match to in vitro enzyme activity of Rubisco can be obtained by considering the mesophyll conductance to CO_2 to the site of carboxylation (Rogers et al., 2001; Flexas et al., 2007); however, as g_m values are available for so few of the sampled species, we assumed that C_i is equal to C_c, the CO_2 concentration at the chloroplast. The C_i at which photosynthesis is colimited by both carboxylation and RuBP regeneration was calculated for each A–C_i curve based on the apparent V_{cmax}, J_{max} and R_{day} using the C_3 photosynthesis model. As the temperature responses of V_{cmax}, J_{max} and R_{day} are not the focus of our study, we did not

adjust the estimated parameter values to a standard temperature. Therefore, all the parameters were estimated at their corresponding measured leaf temperatures. All parameter fits were carried out using the Levenberg–Marquardt least-squares approach (Levenberg, 1944; Marquardt, 1963); the source code is freely available from GitHub (De Kauwe et al., 2015). Of the 1394 measured A–C_i curves, the data used to estimate V_{cmax} were screened to exclude 'bad' measurement curves based on the traditional A-C_i fitting approach, 'bad' being defined according to the following criteria: (i) if the first obtained measurement was at an ambient CO_2 concentration < 300 or > 400 μmol mol^{-1}; (ii) if the fitted function had $r^2 < 0.9$; or (ii) if the relative error of fitted V_{cmax} values is $> 40\%$. After screening this resulted in 1318 measurements; filtering criteria (i), (ii) and (iii) removed c. 4%, 1% and 1%, respectively. The fitting method used makes no assumption about the C_i value at which the leaf transitions between carboxylation and RuBP regeneration limitations (C_i transition point), but it does use a hyperbolic minimum function to smooth the transition between the carboxylation and RuBP regeneration limitations (Kirschbaum & Farquhar, 1984).

$\hat{V}_{cmax}$ estimation from the one-point method

The main underlying assumption of the one-point method is that leaf net photosynthesis under ambient CO_2 and saturated irradiance conditions is limited by Rubisco carboxylation rather than by RuBP regeneration (Rogers & Humphries, 2000; Wilson et al., 2000). As such, $\hat{V}_{cmax}$ can be estimated from the carboxylation-limited portion of the photosynthetic CO_2 response curve, given by:

$$\hat{V}_{cmax} = (A_{sat} + R_{day}) \frac{(C_i + K_m)}{(C_i - \Gamma^*)} \quad \text{(Eqn 1)}$$

where K_m is the Michaelis–Menten constant, given by:

$$K_m = K_c \left(1 + \frac{O_i}{K_0} \right) \quad \text{(Eqn 2)}$$

K_c, K_o (and Γ^*) were estimated following the equations in Table 2. We used the first measurement point of each A–C_i curve as the A_{sat} value required to estimate V_{cmax}. One difficulty with this approach is that it requires an estimate of R_{day}. In the first instance, we used the fitted value for R_{day} obtained from the A–C_i

Table 2 Three sets of temperature dependencies for the Michaelis constant for CO_2 (K_c, µmol mol^{-1}) and the Michaelis constant for O_2 (K_o, mmol mol^{-1}) and the CO_2 compensation point (Γ^*, µmol mol^{-1})

Reference	Badger & Collatz (1977)	Bernacchi *et al.* (2001)	Crous *et al.* (2013)
Environment	*In vivo*	*In vivo*	*In vitro*
Species	Bracted orache (*Atriplex glabriuscula*)	Tobacco (*Nicotiana tabacum*)	Tasmanian blue gum (*Eucalyptus globulus*)
K_c	If $T_k > 288.15$: $460 \cdot \exp\left(\frac{59536(T_k-298.15)}{298.15 \cdot R \cdot T_k}\right)$ else if $T_k < 288.15$: $920 \cdot \exp\left(\frac{10970(T_k-298.15)}{298.15 \cdot R \cdot T_k}\right)$	$404.9 \cdot \exp\left(\frac{79403(T_k-298.15)}{298.15 \cdot R \cdot T_k}\right)$	Same as Bernacchi *et al.* (2001)
K_o	$330 \cdot \exp\left(\frac{35948(T_k-298.15)}{298.15 \cdot R \cdot T_k}\right)$	$278.4 \cdot \exp\left(\frac{36380(T_k-298.15)}{298.15 \cdot R \cdot T_k}\right)$	Same as Bernacchi *et al.* (2001)
Γ^*	$\frac{K_c \cdot O_i \cdot 0.21}{2 \cdot K_o}$	$42.75 \cdot \exp\left(\frac{37830(T_k-298.15)}{298.15 \cdot R \cdot T_k}\right)$	$38.892 \cdot \exp\left(\frac{20437(T_k-298.15)}{298.15 \cdot R \cdot T_k}\right)$

T_k, leaf temperature in Kelvin; R, universal gas constant (8.314 J mol^{-1} K^{-1}); O_i, intercellular concentrations of O_2 (210 mmol mol^{-1}).

curve (hereafter called 'known' R_{day}). This approach may be viewed as a 'best case' test of the method, as these values will not be known when only A_{sat} is measured. In order to estimate V_{cmax} in the situation where R_{day} is not known, we assumed that R_{day} was 1.5% of V_{cmax} (hereafter called 'estimated' R_{day}), following Collatz *et al.* (1991). Under this assumption, the estimation equation is:

$$\hat{V}_{cmax} = A_{sat}\left(\frac{C_i + K_m}{C_i - \Gamma^*} - 0.015\right) \quad \text{(Eqn 3)}$$

The fixed proportion between R_{day} and V_{cmax} was proposed by Collatz *et al.* (1991) to hold at 25°C. We further assumed that this ratio would remain constant with varying leaf temperature, thus assuming similar temperature dependencies for R_{day} and V_{cmax}. This assumption is reasonable because leaf respiration and V_{cmax} both typically have increasing temperature dependencies with Q10 values close to 2 at temperatures up to 35°C (Collatz *et al.*, 1991; Medlyn *et al.*, 2002a,b; Atkin *et al.*, 2015).

Assessing the robustness of the one-point method

We compared $\hat{V}_{cmax}$ values with V_{cmax} values estimated from each full A–C_i curve in order to assess the performance of the one-point method. We also analysed the residuals as a function of a range of variables to identify the circumstances under which the method is most (or least) successful.

As there were 1318 data points, we opted in a number of comparison plots to group (colour) species by PFT, and also to bin these data (Figs 2, S1, S2, and see later Figs 4, 5, 7). Binning the data (with all values within a 'bin' being averaged out to a single value) allows us to better visualize the underlying main trends in large datasets, rather than being distracted by the small number of points towards the edges of any bivariate distribution. Regression lines, however, were fitted to raw data, not to the binned data. Bin sizes are shown in all figure captions.

Other datasets

Using 0.5° resolution Climate Research Unit climatology data (CRU CL1.0; New *et al.*, 1999) over the period 1961–1990, we derived the following for each site: mean annual temperature (MAT; a proxy for growth temperature); mean annual precipitation (MAP); a moisture index (representing an indirect estimate of plant water availability, calculated as the ratio of mean annual precipitation to the equilibrium evapotranspiration, as described in Gallego-Sala *et al.* (2010)); and the number of growing degree-days above 0 and 5°C, respectively. We also obtained site elevation estimates from data from the Advanced Spaceborne Thermal Emission and Reflection Radiometer (ASTER) Global Digital Elevation Model Version 2 (GDEM V2) at 1.0° resolution.

Results

The C_i transition point of each A–C_i curve was located by fitting both the Rubisco- and RuBP-limited net CO_2 assimilation rates and then identifying the point at which the two limitations intersected (transition point) (Fig. 2a). In our dataset, *c.* 94% of the measured A_{sat} values were found to be Rubisco-limited under saturated irradiance and ambient CO_2. This result supports the key underlying assumption of the one-point approach: that in field datasets at current C_a and (importantly) at light saturation, carboxylation usually limits A (hypothesis 1). Among the wide range in estimated transition points there was some distinct patterning according to PFT (Fig. 2b), namely, higher median transition points for evergreen needleleaf species than in broadleaf species (whether evergreen or deciduous; *post hoc* Tukey tests, $P < 0.001$), and higher median transition points in herbaceous species than in deciduous shrubs (*post hoc* Tukey test, $P = 0.08$) (note the deciduous needleleaf forests PFT only has three sample curves).

Known R_{day}

When R_{day} was known, $\hat{V}_{cmax}$ values were in excellent agreement with V_{cmax} derived from traditional A–C_i curve fitting (Fig. 3). Across all species, $\hat{V}_{cmax}$ values were estimated with a positive bias of 0.99 µmol m^{-2} s^{-1}, $r^2 = 0.98$ and RMSE = 8.19 µmol m^{-2} s^{-1}. Error and bias varied somewhat among PFTs (bias = −4.02 to −2.26 µmol m^{-2} s^{-1}, $r^2 > 0.95$, RMSE: 4.33–10.34 µmol m^{-2} s^{-1}) but were still rather modest even in the worst-case, deciduous shrubs (RMSE = 10.34 µmol m^{-2} s^{-1}).

Residuals between V_{cmax} and $\hat{V}_{cmax}$ were examined as a function of several factors, namely: V_{cmax} estimated from traditional A–C_i curves (Fig. 4a), ambient g_s (Fig. 4c), estimated R_{day} (via A–C_i curve; Fig. 4e) and ambient C_i (Fig. 4g); leaf temperature, MAT (a proxy for growth temperature) and MAP (Fig. 5); and a selection of other common indices of site climate (site moisture index, elevation, growing degree-days; Figs S2, S3). The plot of residuals against the 'true' V_{cmax} values (Fig. 4a) shows considerable scatter in individual $\hat{V}_{cmax}$ values. When using a known R_{day}, this spread in errors largely disappears in the binned data, suggesting that it results from a small number of individual measurements. There was a positive trend in the residuals that indicates increasing error with increasing V_{cmax} values, but importantly, most (c. 90% of binned data) errors are small (within 10%, denoted by dotted lines in Fig. 4a).

We originally hypothesized that we would observe larger biases between $\hat{V}_{cmax}$ and V_{cmax} at high ambient C_i and in species sampled from very wet and/or humid environments, as a result of a greater stomatal aperture (hypothesis 1a). When using a known R_{day}, our dataset did not support this hypothesis (Fig. 4c); at high g_s, there was a weak trend for overestimation of V_{cmax}, rather than the hypothesized underestimation expected if the error resulted from being above the operating C_i. Whilst there was a small trend with MAP, the slope was negligible (Fig. 5c) and there were no trends when examining the residuals as a function of C_i (Fig. 4g). We also hypothesized that we might see greater bias at high growth temperatures (hypothesis 1b). When using a known R_{day}, our results do indeed show a significant trend with increasing MAT (proxy for growth temperature; Fig. 5c), and the annual number of growing degree-days (Fig. S3), but again the slope of this trend was negligible. We also hypothesized that we
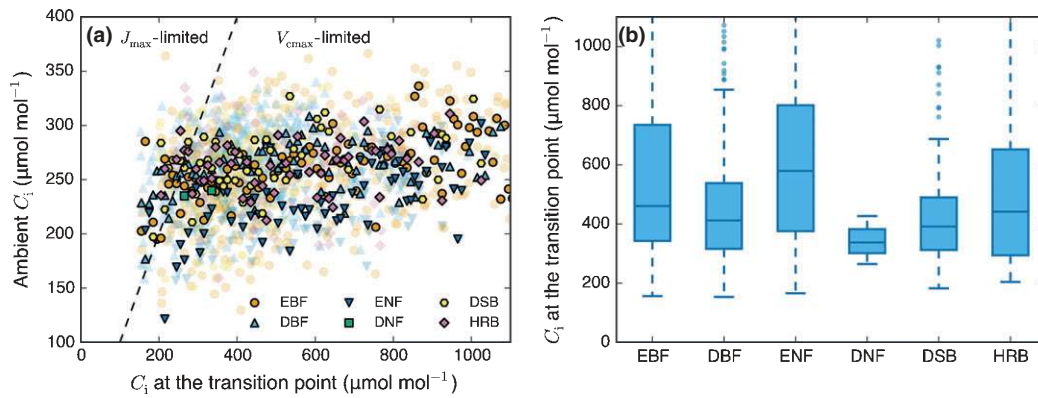

Fig. 2 Relationship between the ambient intercellular CO_2 concentration (C_i) and the C_i value at the transition point obtained from A–C_i curve (net photosynthesis, A, vs intercellular CO_2 concentration, C_i fitting. In panel (a), data shown are for individual species, but have been grouped (coloured) by plant functional type: EBF, evergreen broadleaved forest; DBF, deciduous broadleaved forest; ENF, evergreen needle-leaved forest; DNF, deciduous needle-leaved forest; DSB, deciduous shrubs; HRB, herbaceous species. The data have also been binned (bin size = 10), with the original data shown in a matching semitransparent colour. In panel (b) the box-and-whisker plots show the C_i value at the transition point (line, median; box, interquartile range), with bars extending to 1.5 times the interquartile range. Dots outside of the box and whiskers show outlying points.
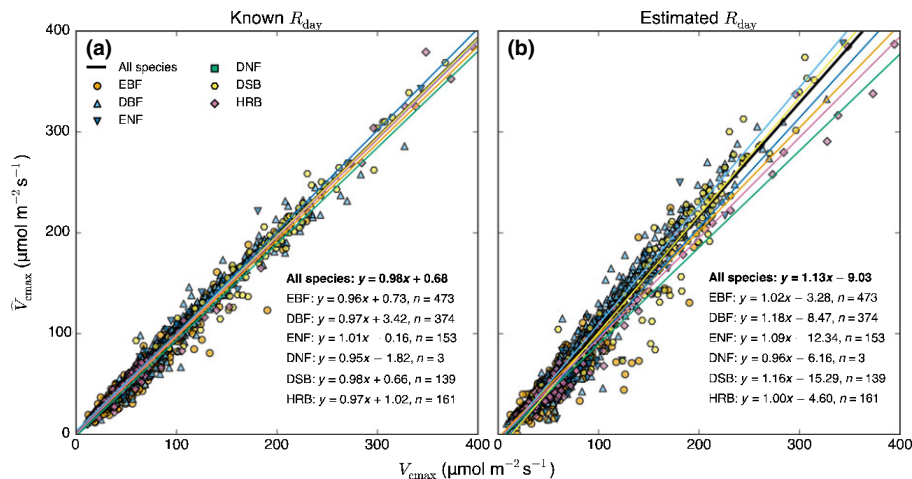

Fig. 3 Comparison between values of the maximum carboxylation rate (V_{cmax}) estimated from traditional A–C_i curve (net photosynthesis, A, vs intercellular CO_2 concentration, C_i) fitting and V_{cmax} estimated from one-point method, $\hat{V}_{cmax}$. Panels (a) and (b) show the effect of using a known and an estimated day respiration (R_{day}) (1.5% of V_{cmax}), respectively. Data shown are for all 1318 species but have been coloured to match representative plant functional types. EBF, evergreen broadleaved forest; DBF, deciduous broadleaved forest; ENF, evergreen needle-leaved forest; DNF, deciduous needle-leaved forest; DSB, deciduous shrubs; HRB, herbaceous species. Regression lines have been fitted to the raw data (1318 species measurements) and coloured to match plant functional types.
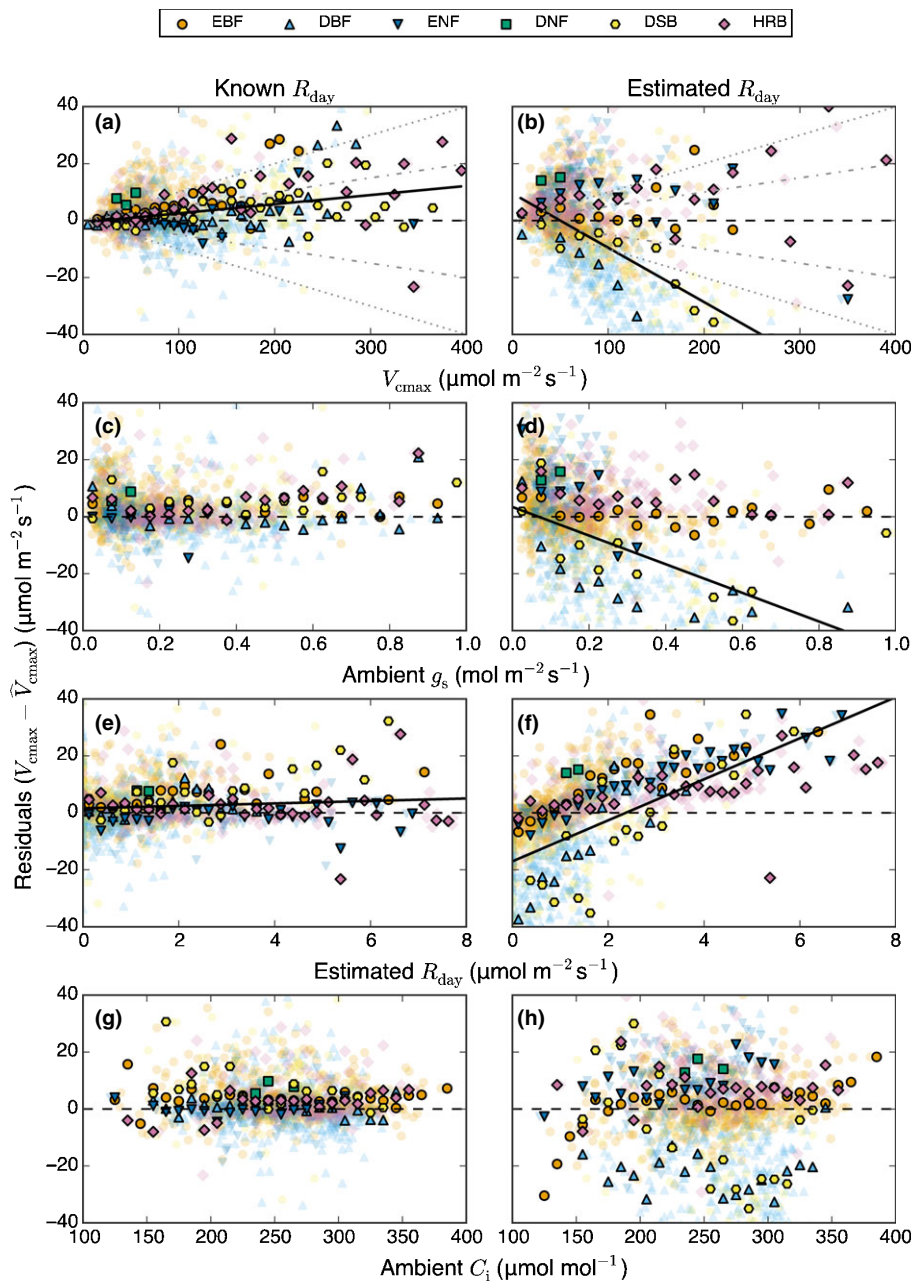
Fig. 4 Residuals (maximum carboxylation rate, V_{cmax}, estimated from one-point method, $\hat{V}_{cmax}$) shown as a function of V_{cmax}, ambient stomatal conductance (g_s), estimated day respiration (R_{day}) and the intercellular CO_2 concentration (C_i). Data were binned (a, b, bin size = 10; c, d, bin size = 0.05; e, f, bin size = 0.25; g, h, bin size = 10), with the original data shown in a matching semitransparent colour. Data shown are for all 1318 species but have been coloured to match representative plant functional types. EBF, evergreen broadleaved forest; DBF, deciduous broadleaved forest; ENF, evergreen needle-leaved forest; DNF, deciduous needle-leaved forest; DSB, deciduous shrubs; HRB, herbaceous species. A significant ($P < 0.05$) trend in the residuals is shown by a solid black line. Trend lines have been fit to the raw data (1318 species measurements). In panels (a) and (b) the grey dashed lines represent 5% (dot-dash) and 10% (dot-dot) error, respectively.

may see larger error (both absolute and relative) in the residuals at low g_s values as a result of a low signal-to-noise ratio (hypothesis 2). To test this prediction, we divided the measurements into two groups: those at low g_s (< 0.2 mol m^{-2} s^{-1}) and those at higher g_s (> 0.2 mol m^{-2} s^{-1}). The RMSE was similar in both groups (8.07 vs 8.37 µmol m^{-2} s^{-1} at low and high g_s, respectively), but the percentage error was greater (8.4% vs 4.5%), supporting our prediction.

Estimated R_{day}

Errors were noticeably greater when R_{day} was estimated as a fixed fraction of V_{cmax}. Overall (all species) there was a negative bias: -2.2 µmol m^{-2} s^{-1}, $r^2 = 0.95$, RMSE $= 17.1$ µmol m^{-2} s^{-1}. When grouping by PFT these errors were further increased

(biases -8.18–10.93 µmol m^{-2} s^{-1}, $r^2 > 0.85$, RMSE: 8.30–26.46 µmol m^{-2} s^{-1}). Examining the residuals between V_{cmax} and $\hat{V}_{cmax}$ as a function of the 'true' V_{cmax} values (Fig. 4b) showed a negative trend, suggesting an overestimation of V_{cmax} at higher values. Errors were at their greatest for species grouped into the deciduous broadleaf forest PFT; here, $\hat{V}_{cmax}$ values are systematic overestimates.

These results provide strong support for the hypothesis that uncertainties in R_{day} would contribute to bias in estimating V_{cmax} values (hypothesis 3). Overall, errors were greater across all comparisons when using an estimated R_{day} than when using a known R_{day}. $\hat{V}_{cmax}$ values also showed a positive trend with increasing R_{day} (Fig. 4f), suggesting a modest but systematic underestimation of $\hat{V}_{cmax}$ at R_{day} values < 2 µmol m^{-2} s^{-1}, and an overestimation at higher R_{day} values.
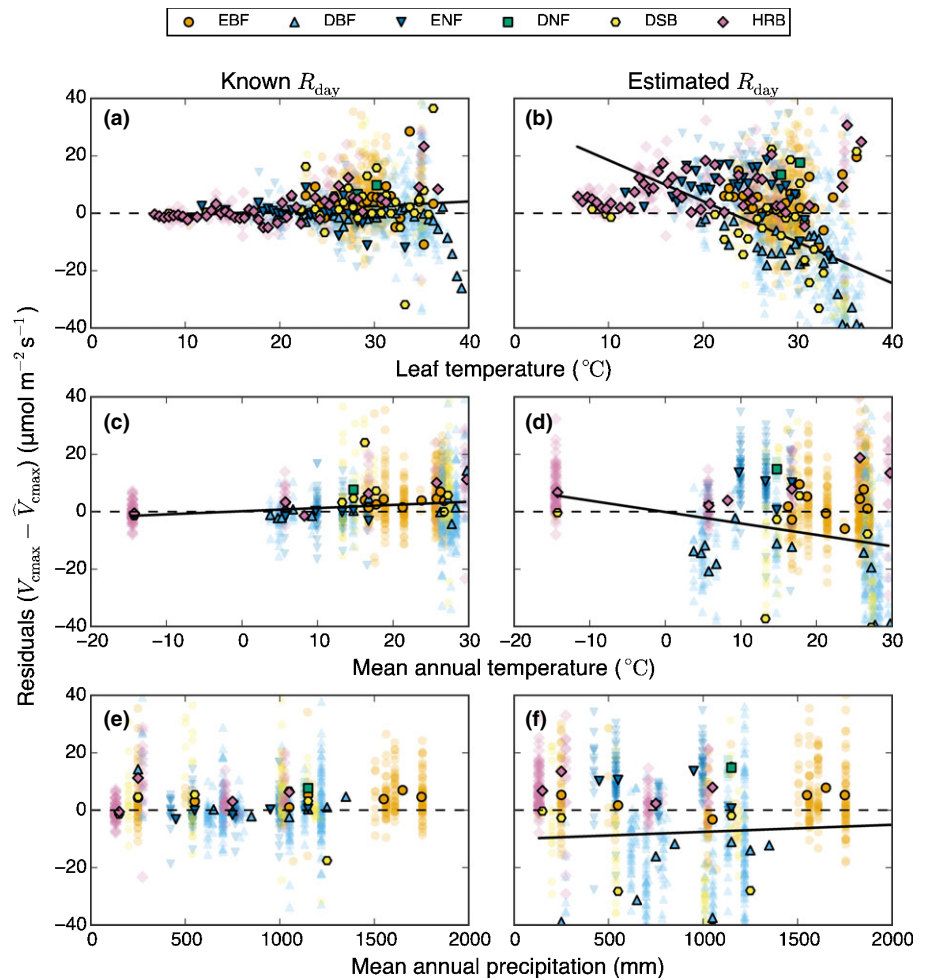
Fig. 5 Residuals (maximum carboxylation rate, V_{cmax}, estimated from one-point method, $\hat{V}_{cmax}$) shown as a function of leaf temperature, mean annual temperature and mean annual precipitation. Data in the residual panels have been binned (a–d, bin size = 0.5; e, f, bin size = 100), with the original data shown in a matching semitransparent colour. Data shown are for all 1318 species, but have been coloured to match representative plant functional types. EBF, evergreen broadleaved forest; DBF, deciduous broadleaved forest; ENF, evergreen needle-leaved forest; DNF, deciduous needle-leaved forest; DSB, deciduous shrubs; HRB, herbaceous species. A significant ($P < 0.05$) trend in the residuals is shown by a solid black line. Trend lines have been fitted to the raw data (1318 species measurements).

To enable the estimation of V_{cmax} without an independent estimate of R_{day}, we assumed a fixed relationship with V_{cmax} that is commonly used in TBMs. However, there was a strong negative relationship between V_{cmax}–$\hat{V}_{cmax}$ residuals and leaf temperature (Fig. 5b) and a notable positive trend in errors with increasing estimates of R_{day} (Fig. 4f), both of which suggest that the relationship between R_{day} and V_{cmax} is not constant. Fig. 6(a) shows the $R_{day} : V_{cmax}$ ratio obtained from fitting our A–C_i response curves as a function of leaf temperature for the B01 temperature dependencies for K_c, K_o and Γ^*. The data show a strong negative trend with increasing temperature. This strong negative trend arises because the fitted R_{day} values decline with leaf temperature (Fig. 6b), rather than increasing in line with V_{cmax} as we assumed. Fig. 6(b) indicates that fitted R_{day} values commonly hit the lower bound of zero above 25°C. As R_{day} is estimated as the value of A where $C_i = \Gamma^*$, and this may indicate that the values of Γ^* used are inappropriate for these datasets.

Sensitivity to temperature dependencies of K_c, K_o and Γ^*

We repeated the exercise of comparing $\hat{V}_{cmax}$ and V_{cmax} using two alternative temperature dependencies of K_c, K_o and Γ^* for the case where R_{day} was estimated (Figs 7, S4, S5). The accuracy of estimated values was largely insensitive to our three tested

assumptions. $\hat{V}_{cmax}$ values estimated with the C13 parameterization had the lowest RMSE values (average across all PFTs = 13.85 μmol m^{-2} s^{-1}) and those estimated with BC77 had the largest (average across all PFTs = 15.42 μmol m^{-2} s^{-1}). However, grouping by PFTs, the mean absolute difference between the different parameterizations was small, c. 2 μmol m^{-2} s^{-1}. It is also notable that using the BC77 parameterization resulted in greater errors for herbaceous species (RMSE = c. 19 vs c. 11 μmol m^{-2} s^{-1} for B01 and C13 parameterizations). Figs S4 and S5 demonstrate that the assumption of a fixed ratio of 0.015 for $R_{day} : V_{cmax}$ is still relatively poor for BC77 and C13 parameterizations, particularly at low leaf temperatures; the approximation is marginally better for the C13 parameterization, explaining the lower RMSE values obtained with this parameterization.

Discussion

In this study we have examined an alternative approach to traditional A–C_i curve analysis for estimating V_{cmax}, an approach that holds promise for greatly expanding the set of species represented in global V_{cmax} datasets. One of the principal concerns about the use of this approach has been that typical measurements of A_{sat} may be limited by RuBP regeneration rates, rather than Rubisco activity, and hence would yield underestimates of V_{cmax},
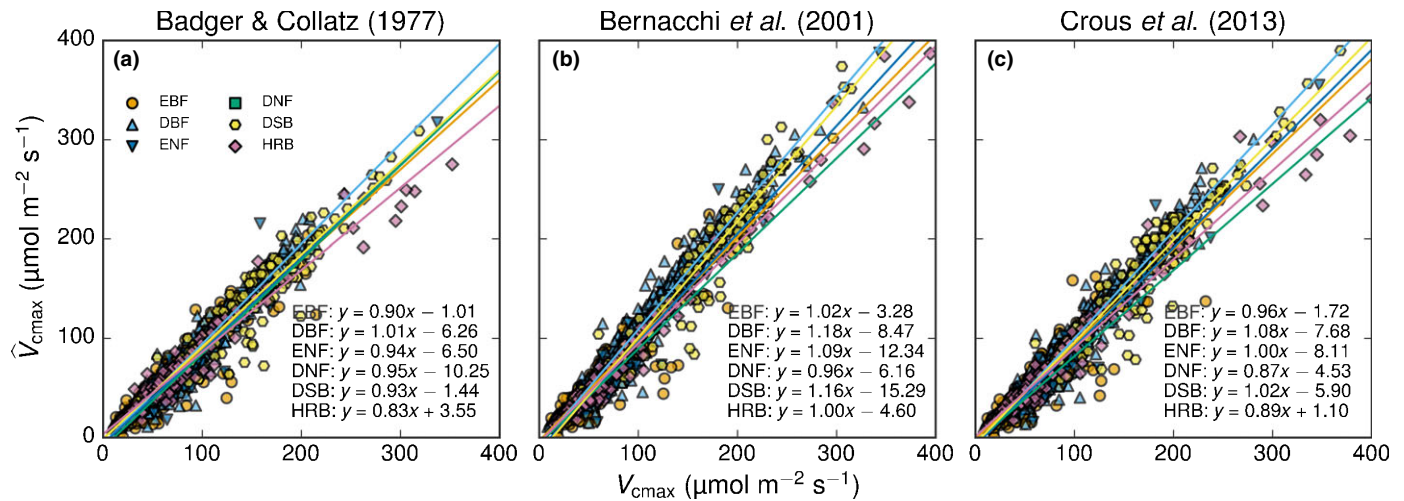
Fig. 6 Relationship between values of the maximum carboxylation rate (V_{cmax}) estimated from the traditional approach and V_{cmax} estimated from the one-point method ($\hat{V}_{cmax}$) using three different sets of the Michaelis constant for CO_2 (K_c), the Michaelis constant for O_2 (K_o), and the CO_2 compensation point in the absence of mitochondrial respiration (Γ^*) parameters. Data shown are for all 1318 species, but have been coloured to match representative plant functional types. EBF, evergreen broadleaved forest; DBF, deciduous broadleaved forest; ENF, evergreen needle-leaved forest; DNF, deciduous needle-leaved forest; DSB, deciduous shrubs; HRB, herbaceous species. Regression lines have been fitted to the raw data (1318 species measurements) and coloured to match plant functional types.
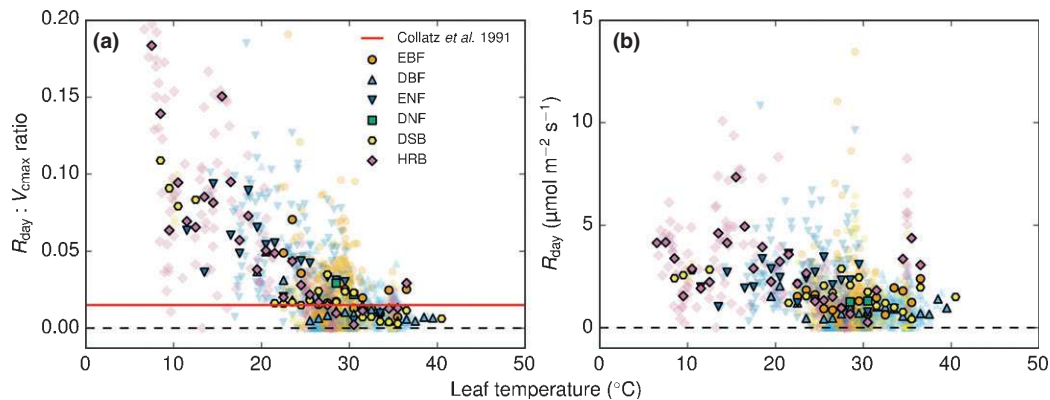

Fig. 7 (a, b) Fitted day respiration : maximum carboxylation rate ($R_{day} : V_{cmax}$) ratio (a) and R_{day} (b) as a function of leaf temperature using the Bernacchi et al. (2001) parameters. Data shown are for all 1318 species, but have been coloured to match representative plant functional types. EBF, evergreen broadleaved forest; DBF, deciduous broadleaved forest; ENF, evergreen needle-leaved forest; DNF, deciduous needle-leaved forest; DSB, deciduous shrubs; HRB, herbaceous species. The horizontal red line shows the $R_{day} : V_{cmax}$ commonly assumed by terrestrial biosphere models following Collatz et al. (1991).

especially in wet or warm conditions. Here we have demonstrated that, for photosynthesis measurements taken at ambient CO_2 and under saturating irradiance conditions, values are normally Rubisco-limited and, as such, $\hat{V}_{cmax}$ values are in good agreement with V_{cmax} determined from $A–C_i$ curves. Residual analysis when using a known R_{day} did not show any bias in V_{cmax} estimation with environmental conditions such as MAT or MAP. Because of this, our results suggested that the one-point method is likely to be a robust means to resolve V_{cmax} from light-saturated photosynthesis.

That said, our analysis did identify other, nontrivial sources of error in using the one-point approach. First, we found support for our hypothesis that increased errors would occur at low g_s as a result of a lower signal-to-noise ratio (hypothesis 2), suggesting that rates of A_{sat} that are not subject to severe stomatal limitation are most suited to this approach. Second, poor estimation of R_{day}

led to a notable increase in the RMSE of estimates, approximately doubling RMSE from 7.18 to 14.71 $\mu mol\ m^{-2}\ s^{-1}$. The proportional error in V_{cmax} when estimating R_{day} (i.e. Fig. 4b) was, on average, c. 20% for most datasets when grouped by PFT. These errors were larger because we estimated R_{day} using a fixed $R_{day} : V_{cmax}$ relationship, and this relationship did not capture variation in values of fitted R_{day}. There was strong bias at low and high temperatures, leading to a clear pattern in residuals. In addition, there was higher estimation error ($V_{cmax}–\hat{V}_{cmax}$ residuals) at higher V_{cmax}, higher leaf temperatures or at hotter sites (although it should be noted V_{cmax} is typically greater at higher temperatures), and at either very high or very low R_{day}. Having identified and quantified these apparently systematic biases, it would then, of course, be up to individual researchers using this method to decide for themselves what magnitude of error (or bias) was acceptable for the purpose at hand.

R_{day} is as yet not well understood in terms of responses to environmental variation or temperature dependence and hence is difficult to model (Tcherkez *et al.*, 2012; Heskel *et al.*, 2013; Way & Yamori, 2014). It is widely understood that estimates of R_{day} obtained from A–C_i curves are inaccurate. One reason for the inaccuracy is that the values are extrapolated from small fluxes at low C_i conditions, and hence are subject to noise and possibly gasket-leak effects (Bruhn *et al.*, 2002; Hurry *et al.*, 2005). In this study we also show that there is a systematic bias in R_{day} estimates with temperature (Figs 5, 6), which leads to bias in estimates of $\hat{V}_{cmax}$. This bias could potentially result from a number of factors. First, fluxes are lower at lower temperature, so errors as a result of noise may be greater. Second, it is likely that our assumptions for the temperature dependence of either R_{day} or Γ^*, or both, are incorrect. Fitted estimates of R_{day} showed either no temperature dependence or a negative temperature dependence, depending on what Γ^* was assumed (Figs 6, S4, S5). By contrast, most studies of R_{day} suggest a positive temperature dependence, as is assumed in most TBMs (Clark *et al.*, 2011; Heskel *et al.*, 2013). The issue may lie with Γ^*; the most widely used parameterization for Γ^* (B01) resulted in fitted values of R_{day} going to zero at higher temperatures, suggesting this parameterization may in fact be too temperature-sensitive for many species. This issue also affects photosynthesis values estimated by TBMs using estimates of V_{cmax} obtained from A–C_i curves, because such models commonly use a fixed ratio for $R_{day} : V_{cmax}$. The estimates of V_{cmax} are dependent on the fitted values of R_{day} (i.e. our known R_{day}). If models estimate photosynthesis with fitted V_{cmax} but a fixed $R_{day} : V_{cmax}$ ratio, the resulting estimates of photosynthesis will be in error. Addressing this problem requires that we develop better empirical parameterizations of the temperature dependencies of both Γ^* and R_{day}, which are applicable across species and climates, rather than the single-species, single-site relationships currently used.

An alternative approach to using a fixed $R_{day} : V_{cmax}$ ratio would be to base estimates of R_{day} on measured values of dark respiration rate, R_{dark}. For example, it could be assumed that $R_{day} = 0.6 \times R_{dark}$ (Kirschbaum & Farquhar, 1984) or, alternatively, one might simply set $R_{day} = R_{dark}$, as was done by Atkin *et al.* (2015) when employing the one-point method. However, we note that such approaches would still result in errors when estimating $\hat{V}_{cmax}$, because they both assume a similar temperature dependence for R_{day} and R_{dark}, whereas the fitted temperature dependence of R_{day} does not resemble the exponential response typically found for R_{dark} (Figs 6, S4, S5).

New research avenues

Despite the error introduced by inaccuracies in R_{day}, the one-point method nevertheless has the potential to provide new insight into variability of apparent V_{cmax} across and within species, PFTs and in relation to other plant traits. Owing to logistical constraints, studies estimating apparent V_{cmax} using A–C_i curves typically focus on a relatively small number of species, and are biased towards both controlled environments and temperate regions (Wullschleger, 1993; Kattge *et al.*, 2009; Sun *et al.*, 2014; Walker

et al., 2014). The results of this paper suggest that measurements of A_{sat}, which are more readily made on a wide range of species under field conditions, can also be used to estimate V_{cmax} using the one-point method. An expanded global V_{cmax} database would greatly facilitate testing of ecophysiological theories of plant trait distribution based on environmentally driven traits (Verheijen *et al.*, 2013; van Bodegom *et al.*, 2014; Reich *et al.*, 2014), trait tradeoffs (Wright *et al.*, 2010; Reu *et al.*, 2011) and optimality concepts (Xu *et al.*, 2012; Prentice *et al.*, 2014; Wang *et al.*, 2014; Ali *et al.*, 2015b). Larger datasets for V_{cmax} would also allow insights into the true scaling of photosynthetic capacity with leaf structural and chemical traits, with the caveat that we have identified some systematic biases in the approach, suggesting it would be best to constrain analysis to data < 30°C (Fig. 5b).

From a modelling perspective, additional data would serve to improve the underlying evidence base used to constrain model simulations of photosynthesis. For example, Bonan *et al.* (2011) found that uncertainty as a result of V_{cmax} was equivalent to uncertainties arising from structural errors (e.g. scaling photosynthesis and stomatal conductance from the leaf to the canopy), accounting for a *c.* 30 Pg C yr^{-1} variation in modelled gross primary productivity in CLM4. A number of models (e.g. CABLE, JULES, CLM4) assume that the J_{max} parameter and/or the autotrophic respiration are proportional to V_{cmax}. Therefore, this single parameter has a marked impact on modelled carbon flux, and improvements in the V_{cmax} parameter have the potential to constrain multiple facets of current TBMs. For example, Dietze *et al.* (2014) showed that inclusion of even small observational datasets of V_{cmax} could adequately constrain the parameterization of the ecosystem demography (ED2) model across a range of biomes. Furthermore, it is now commonplace in some modelling studies to simulate vegetation fluxes considering the full uncertainty of key parameters, rather than assuming a PFT can be described by a single value (Ziehn *et al.*, 2011; Wang *et al.*, 2012).

It should be noted that our analysis calls into question the modelling assumption that J_{max} is proportional to V_{cmax}, as shown by the high variability in C_i transition points observed across our dataset (Fig. 2). These transition points can be used to estimate the ratio of $J_{max} : V_{cmax}$. We estimated this ratio at 25°C from the transition points, and found a mean value of 1.9 with a large interquartile range, stretching from 1.68 to 2.14. As noted earlier, there was some difference in the median transition point (and hence $J_{max} : V_{cmax}$ ratio) among PFTs, but the variability within a PFT is considerably larger than that between PFTs. While the one-point method can provide insights into variation in V_{cmax}, it does not enable us to develop better parameterizations for other key photosynthetic parameters. There remains a need for full A–C_i curves to also quantify the variability in $J_{max} : V_{cmax}$ ratio, or, as an alternative, cluster sampling approaches (e.g. extensively sampling of the photosynthesis-light response curve) as proposed by Dietze (2014).

There is also the potential for a complementary set of parameter estimates to be obtained through a re-examination of existing A_{sat} datasets. Large quantities of field-measured A_{sat} data currently exist in global databases, for example *c.* 1500 species in Maire *et al.* (2015) and 2192 species in TRY (Kattge *et al.*,

2011). By putting together V_{cmax} data derived from A–C_i curves with V_{cmax} values determined from the one-point method (i.e. $\hat{V}_{cmax}$), there is the potential to generate a database consisting of data for thousands of species, for many hundred sites around the world. Consistent conversion of A_{sat} to V_{cmax} values in worldwide datasets would be strongly beneficial, enabling a wider characterization of V_{cmax} variations across the globe, and better quantification of relationships between V_{cmax} and other leaf traits (Walker et al., 2014) and with site climate (Ali et al., 2015a,b). However, it is important to note that application of the one-point method to these datasets may involve additional sources of error. For example, Kattge et al. (2009) estimated $\hat{V}_{cmax}$ using a one-point method applied to A_{sat} data that did not include complementary values of C_i, and thus estimated C_i as a constant fraction (0.8) of C_a. In our dataset, the 25th and 75th quartiles for the $C_i : C_a$ ratio were 0.60–0.75; use of a constant value would thus have introduced considerable additional error. Application of the one-point method to species-mean values of A_{sat} and g_s, such as those collated by Maire et al. (2015), would also be subject to systematic error from averaging a nonlinear function. Thus, application of the one-point method in these circumstances needs to be done with caution.

This manuscript presents an empirical justification for using the one-point method, which we conclude can be used to estimate accurate values of V_{cmax}, for an estimate that we labelled $\hat{V}_{cmax}$ for distinction from intensively measured curves. We stress that continued measurement of plant behaviour using detailed A–C_i response curves is still invaluable and, indeed, 'best practice'. Fitting the model of Farquhar et al. (1980) to data has provided a tried and tested means to evaluate and interpret plant physiological behaviour in the field and laboratory alike. The one-point method tested here complements the traditional approach, potentially allowing us to greatly expand plant trait datasets of maximum carboxylation efficiency.

Author contributions

I.J.W., V.M., Y-S.L., D.S.E., B.E.M., I.C.P., Ü.N., O.K.A. and B.J.E. planned and designed the research. M.G.D.K. and Y-S.L. performed all research and data analysis. K.Y.C, D.S.E, V.M., O.K.A, A.R., Ü.N., S.P.S., P.M., J.U., H.F.T., L.T., L.K.W., F.Y.I. and T.F.D measured all the field data used in the experiment. M.G.D.K., I.J.W., B.E.M., K.Y.C, D.S.E, V.M., I.C.P. and Y-S.L. wrote the first draft; all authors commented on subsequent versions and assisted with data interpretation.

References

del Aguila-Pasquel J, Doughty CE, Metcalfe DB, Silva-Espejo JE, Girardin CA, Chung Gutierrez JA, Navarro-Aguilar GE, Quesada CA, Hidalgo CG, Reyna Huaymacari JM *et al.* 2014. The seasonal cycle of productivity, metabolism and carbon dynamics in a wet aseasonal forest in north-west Amazonia (Iquitos, Peru). *Plant Ecology & Diversity* 7: 71–83.

Ali AA, Xu C, Rogers A, Fisher RA, Wullschleger SD, McDowell NG, Massoud EC, Vrugt JA, Muss JD, Fisher JB *et al.* 2015b. A global scale mechanistic model of the photosynthetic capacity. *Geoscientific Model Development Discussions* 8: 6217–6266.

Ali AA, Xu C, Rogers A, McDowell NG, Medlyn BE, Fisher RA, Wullschleger SD, Reich PB, Vrugt JA, Bauerle WL *et al.* 2015a. Global scale environmental control of plant photosynthetic capacity. *Ecological Applications* 25: 2349–2365.

Anderson L, Malhi Y, Ladle R, Aragao L, Shimabukuro Y, Phillips O, Baker T, Costa A, Espejo J, Higuchi N *et al.* 2009. Influence of landscape heterogeneity on spatial patterns of wood productivity, wood specific density and above ground biomass in Amazonia. *Biogeosciences* 6: 1883–1902.

Atkin OK, Bloomfield KJ, Reich PB, Tjoelker MG, Asner GP, Bonal D, Bönisch G, Bradford M, Cernusak LA, Cosio EG *et al.* 2015. Global variability in leaf respiration in relation to climate, plant functional types and leaf traits. *New Phytologist* 206: 614–636.

Badger MR, Collatz GJ. 1977. Studies on the kinetic mechanism of RuBP carboxylase and oxygenase reactions, with particular reference to the effect of temperature on kinetic parameters. *Year book–Carnegie Institution of Washington* 76: 355–361.

Bernacchi C, Singsaas E, Pimentel C, Portis A Jr, Long S. 2001. Improved temperature response functions for models of Rubisco-limited photosynthesis. *Plant, Cell & Environment* 24: 253–259.

Beer C, Reichstein M, Tomelleri E, Ciais P, Jung M, Carvalhais N, Rodenbeck C, Atlaf Arain M, Baldocchi D, Bonan GB *et al.* 2010. Terrestrial gross carbon dioxide uptake: global distribution and covariation with climate. *Science* 329: 834–838.

van Bodegom PM, Douma JC, Verheijen LM. 2014. A fully traits-based approach to modeling global vegetation distribution. *Proceedings of the National Academy of Sciences, USA* **111**: 13733–13738.

Bonan GB, Lawrence PJ, Oleson KW, Levis S, Jung M, Reichstein M, Lawrence DM, Swenson SC. 2011. Improving canopy processes in the Community Land Model version 4 (CLM4) using global flux fields empirically inferred from FLUXNET data. *Journal of Geophysical Research* **116**: G02014.

Brooks A, Farquhar G. 1985. Effect of temperature on the CO_2/O_2 specificity of ribulose-1, 5-bisphosphate carboxylase/oxygenase and the rate of respiration in the light. *Planta* **165**: 397–406.

Bruhn D, Mikkelsen TN, Atkin OK. 2002. Does the direct effect of atmospheric CO_2 concentration on leaf respiration vary with temperature? Responses in two species of *Plantago* that differ in relative growth rate. *Physiologia Plantarum* **114**: 57–64.

von Caemmerer S. 2000. *Biochemical models of leaf photosynthesis. Techniques in plant science, no. 2.* Collingwood, Vic., Australia: CSIRO Publishing.

von Caemmerer S, Farquhar GD, Berry JA. 2009. Biochemical model of C_3 photosynthesis. In: Laisk A, Nedbal L, Govindjee , eds. *Photosynthesis in silico: understanding complexity from molecules to ecosystems.* Dordrecht, the Netherlands: Springer Science + Business Media, 209–230.

Chen J-L, Reynolds JF, Harley PC, Tenhunen JD. 1993. Coordination theory of leaf nitrogen distribution in a canopy. *Oecologia* **93**: 63–69.

Clark DB, Mercado LM, Sitch S, Jones CD, Gedney N, Best MJ, Pryor M, Rooney GG, Essery RLH, Blyth E et al. 2011. The Joint UK Land Environment Simulator (JULES), model description – Part 2: carbon fluxes and vegetation dynamics. *Geoscientific Model Development* **4**: 701–722.

Collatz GJ, Ball JT, Grivet C, Berry JA. 1991. Regulation of stomatal conductance and transpiration: a physiological model of canopy processes. *Agricultural and Forest Meteorology* **54**: 107–136.

Crous K, Reich P, Hunter M, Ellsworth D. 2010. Maintenance of leaf N controls the photosynthetic CO_2 response of grassland species exposed to 9 years of free-air CO_2 enrichment. *Global Change Biology* **16**: 2076–2088.

Crous KY, Quentin AG, Lin Y-S, Medlyn BE, Williams DG, Barton CV, Ellsworth DS. 2013. Photosynthesis of temperate *Eucalyptus globulus* trees outside their native range has limited adjustment to elevated CO_2 and climate warming. *Global Change Biology* **19**: 3790–3807.

De Kauwe MG, Lin Y-S, Medlyn BE. 2015. FitFarquharModel: Vcmax one-point method. *Zenodo*. doi:10.5281/zenodo.30954.

Dietze M. 2014. Gaps in knowledge and data driving uncertainty in models of photosynthesis. *Photosynthesis Research* **119**: 3–14.

Dietze MC, Serbin SP, Davidson C, Desai AR, Feng X, Kelly R, Kooper R, LeBauer D, Mantooth J, McHenry K et al. 2014. A quantitative assessment of a terrestrial biosphere model's data needs across North American biomes. *Journal of Geophysical Research-Biogeosciences* **119**: 286–300.

Domingues TF, Berry JA, Martinelli LA, Ometto JP, Ehleringer JR. 2005. Parameterization of canopy structure and leaf-level gas exchange for an eastern Amazonian tropical rain forest (Tapajos National Forest, Para, Brazil). *Earth Interactions* **9**: 1–23.

Domingues TF, Ishida FY, Feldpausch TR, Grace J, Meir P, Saiz G, Sene O, Schrodt F, Sonké B, Taedoumg H et al. 2015. Biome-specific effects of nitrogen and phosphorus on the photosynthetic characteristics of trees at a forest-savanna boundary in Cameroon. *Oecologia* **178**: 659–672.

Domingues TF, Meir P, Feldpausch TR, Saiz G, Veenendaal EM, Schrodt F, Bird M, Djagbletey G, Hien F, Compaore H et al. 2010. Co-limitation of photosynthetic capacity by nitrogen and phosphorus in West Africa woodlands. *Plant, Cell & Environment* **33**: 959–980.

Dreyer E, Le Roux X, Montpied P, Daudet FA, Masson F. 2001. Temperature response of leaf photosynthetic capacity in seedlings from seven temperate tree species. *Tree Physiology* **21**: 223–232.

Dubois JJB, Fiscus EL, Booker FL, Flowers MD, Reid CD. 2007. Optimizing the statistical estimation of the parameters of the Farquhar–von Caemmerer-Berry model of photosynthesis. *New Phytologist* **176**: 402–414.

Ellsworth DS, Crous KY, Lambers H, Cooke J. 2015. Phosphorus recycling in photorespiration maintains high photosynthetic capacity in woody species. *Plant, Cell & Environment* **38**: 1142–1156.

Ellsworth DS, Reich PB, Naumburg ES, Koch GW, Kubiske ME, Smith SD. 2004. Photosynthesis, carboxylation and leaf nitrogen responses of 16 species

to elevated pCO_2 across four free-air CO_2 enrichment experiments in forest, grassland and desert. *Global Change Biology* **10**: 2121–2138.

Ellsworth DS, Thomas R, Crous KY, Palmroth S, Ward E, Maier C, DeLucia E, Oren R. 2012. Elevated CO_2 affects photosynthetic responses in canopy pine and subcanopy deciduous trees over 10 years: a synthesis from Duke FACE. *Global Change Biology* **18**: 223–242.

Evans J. 1986. The relationship between carbon-dioxide-limited photosynthetic rate and ribulose-1,5-bisphosphate-carboxylase content in two nuclear-cytoplasm substitution lines of wheat, and the coordination of ribulose-bisphosphate-carboxylation and electron-transport capacities. *Planta* **167**: 351–358.

Farquhar G, von Caemmerer S, Berry J. 1980. A biochemical model of photosynthetic CO_2 assimilation in leaves of C_3 species. *Planta* **149**: 78–90.

Feng X, Dietze M. 2013. Scale dependence in the effects of leaf ecophysiological traits on photosynthesis: Bayesian parameterization of photosynthesis models. *New Phytologist* **200**: 1132–1144.

Field CB, Mooney HA. 1986. The photosynthesis-nitrogen relationship in wild plants. In: Givnish TJ, ed. *On the economy of plant form and function.* Cambridge, UK: Cambridge University Press, 22–55.

Flexas J, Ortuño M, Ribas-Carbo M, Diaz-Espejo A, Flórez-Sarasa I, Medrano H. 2007. Mesophyll conductance to CO_2 in *Arabidopsis thaliana*. *New Phytologist* **175**: 501–511.

Friedlingstein P, Meinshausen M, Arora VK, Jones CD, Anav A, Liddicoat SK, Knutti R. 2014. Uncertainties in CMIP5 climate projections due to carbon cycle feedbacks. *Journal of Climate* **27**: 511–526.

Gallego-Sala A, Clark JM, House JI, Orr HG, Prentice IC, Smith P, Farewell T, Chapman SJ. 2010. Bioclimatic envelope model of climate change impacts on blanket peatland distribution in Great Britain. *Climate Research* **45**: 151–162.

Girardin CAJ, Espejob JES, Doughty CE, Huasco WH, Metcalfe DB, Durand-Baca L, Marthews TR, Aragao LE, Farfán-Rios W, García-Cabrera K et al. 2014a. Productivity and carbon allocation in a tropical montane cloud forest in the Peruvian Andes. *Plant Ecology & Diversity* **7**: 107–123.

Girardin CAJ, Malhi Y, Feeley K, Rapp J, Silman M, Meir P, Huaraca Huasco W, Salinas N, Mamani M, Silva-Espejo J et al. 2014b. Seasonality of above-ground net primary productivity along an Andean altitudinal transect in Peru. *Journal of Tropical Ecology* **30**: 503–519.

Grassi G, Vicinelli E, Ponti F, Cantoni L, Magnani F. 2005. Seasonal and interannual variability of photosynthetic capacity in relation to leaf nitrogen in a deciduous forest plantation in northern Italy. *Tree Physiology* **25**: 349–360.

Gu F, Zhang Y, Tao B, Wang Q, Yu G, Zhang L, Li K. 2010. Modeling the effects of nitrogen deposition on carbon budget in two temperate forests. *Ecological Complexity* **7**: 139–148.

Heskel MA, Atkin OK, Turnbull MH, Griffin KL. 2013. Bringing the Kok effect to light: a review on the integration of daytime respiration and net ecosystem exchange. *Ecosphere* **4**: art98.

Hirose T, Werger M. 1987. Maximizing daily canopy photosynthesis with respect to the leaf nitrogen allocation pattern in the canopy. *Oecologia* **72**: 520–526.

Huasco WH, Girardin CA, Doughty CE, Metcalfe DB, Baca LD, Silva-Espejo JE, Cabrera DG, Aragão LE, Davila AR, Marthews TR et al. 2014. Seasonal production, allocation and cycling of carbon in two mid-elevation tropical montane forest plots in the Peruvian Andes. *Plant Ecology & Diversity* **7**: 125–142.

Hunter JD. 2007. Matplotlib: A 2D graphics environment. *Computing in Science & Engineering* **9**: 90–95.

Hurry V, Igamberdiev AU, Keerberg O, Pärnik T, Atkin OK, Zaragoza-Castells J, Gardeström P. 2005. Respiration in photosynthetic cells: gas exchange components, interactions with photorespiration and the operation of mitochondria in the light. In: Lambers H, Ribas-Carbo M, eds. *Plant respiration: from cell to ecosystem. Advances in photosynthesis and respiration, vol. 18.* Dordrecht, the Netherlands: Springer, 43–61.

Jones E, Oliphant E, Peterson P et al. 2001. SciPy: open source scientific tools for Python 2001. http://www.scipy.org/ [accessed 17 December 2015].

Jordan DB, Ogren WL. 1984. The CO_2/O_2 specificity of ribulose 1,5-bisphosphate carboxylase/oxygenase. *Planta* **161**: 308–313.

Kattge J, Diaz S, Lavorel S, Prentice I, Leadley P, Bönisch G, Garnier E, Westoby M, Reich PB, Wright I et al. 2011. TRY–a global database of plant traits. *Global Change Biology* **17**: 2905–2935.

Kattge J, Knorr W. 2007. Temperature acclimation in a biochemical model of photosynthesis: a reanalysis of data from 36 species. *Plant, Cell & Environment* **30**: 1176–1190.

Kattge J, Knorr W, Raddatz T, Wirth C. 2009. Quantifying photosynthetic capacity and its relationship to leaf nitrogen content for global-scale terrestrial biosphere models. *Global Change Biology* **15**: 976–991.

Kirschbaum MU, Farquhar GD. 1984. Temperature Dependence of Whole-leaf Photosynthesis in *Eucalyptus pauciflora* Sieb. Ex Spreng. *Australian Journal of Plant Physiology* **11**: 519–538.

Kosugi Y, Shibata S, Kobashi S. 2003. Parameterization of the CO_2 and H_2O gas exchange of several temperate deciduous broad-leaved trees at the leaf scale considering seasonal changes. *Plant, Cell & Environment* **26**: 285–301.

Levenberg K. 1944. A method for the solution of certain non–linear problems in least squares. *Quarterly Journal of Applied Mathematics* **2**: 164–168.

Lin Y-S, Medlyn BE, De Kauwe MG, Ellsworth DS. 2013. Biochemical photosynthetic responses to temperature: how do interspecific differences compare with seasonal shifts? *Tree Physiology* **33**: 793–806.

Long S, Bernacchi C. 2003. Gas exchange measurements, what can they tell us about the underlying limitations to photosynthesis? Procedures and sources of error. *Journal of Experimental Botany* **54**: 2393–2401.

Maire V, Martre P, Kattge J, Gastal F, Esser G, Fontaine S, Soussana J-F. 2012. The coordination of leaf photosynthesis links C and N fluxes in C_3 plant species. *PLoS ONE* **7**: e38345.

Maire V, Wright IJ, Prentice IC, Batjes NH, Bhaskar R, Bodegom PM, Cornwell WK, Ellsworth D, Niinemets Ü, Ordonez A et al. 2015. Global effects of soil and climate on leaf photosynthetic traits and rates. *Global Ecology and Biogeography* **24**: 706–717.

Malhi Y, Farfán Amézquita F, Doughty CE, Silva-Espejo JE, Girardin CA, Metcalfe DB, Aragão LE, Huaraca-Quispe LP, Alzamora-Taype I, Eguiluz-Mora L et al. 2014. The productivity, metabolism and carbon cycle of two lowland tropical forest plots in south-western Amazonia, Peru. *Plant Ecology & Diversity* **7**: 85–105.

Marquardt DW. 1963. An algorithm for least-squares estimation of nonlinear parameters. *Journal of the Society for Industrial & Applied Mathematics* **11**: 431–441.

Medlyn B, Dreyer E, Ellsworth D, Forstreuter M, Harley P, Kirschbaum M, Le Roux X, Montpied P, Strassemeyer J, Walcroft A et al. 2002a. Temperature response of parameters of a biochemically based model of photosynthesis. II. A review of experimental data. *Plant, Cell & Environment* **25**: 1167–1179.

Medlyn BE, Loustau D, Delzon S. 2002b. Temperature response of parameters of a biochemically based model of photosynthesis. I. Seasonal changes in mature maritime pine (*Pinus pinaster* Ait.). *Plant, Cell & Environment* **25**: 1155–1165.

Meir P, Kruijt B, Broadmeadow M, Barbosa E, Kull O, Carswell F, Nobre A, Jarvis P. 2002. Acclimation of photosynthetic capacity to irradiance in tree canopies in relation to leaf nitrogen concentration and leaf mass per unit area. *Plant, Cell & Environment* **25**: 343–357.

Miao Z, Xu M, Lathrop RG, Wang Y. 2009. Comparison of the A-Cc curve fitting methods in determining maximum ribulose 1·5-bisphosphate carboxylase/oxygenase carboxylation rate, potential light saturated electron transport rate and leaf dark respiration. *Plant, Cell & Environment* **32**: 109–122.

New M, Hulme M, Jones P. 1999. Representing twentieth-century space–time climate variability. Part I: development of a 1961–90 mean monthly terrestrial climatology. *Journal of Climate* **12**: 829–856.

Newville M, Stensitzki T, Allen DB, Ingargiola A. 2014. LMFIT: non-linear least-square minimization and curve-fitting for Python. *Zenodo*. doi.org/10.5281/zenodo.11813.

Niinemets Ü. 1998. Adjustment of foliage structure and function to a canopy light gradient in two co-existing deciduous trees. Variability in leaf inclination angles in relation to petiole morphology. *Trees* **12**: 446–451.

Niinemets Ü. 1999. Components of leaf dry mass per area – thickness and density – alter leaf photosynthetic capacity in reverse directions in woody plants. *New Phytologist* **144**: 35–47.

Niinemets Ü, Díaz-Espejo A, Flexas J, Galmés J, Warren CR. 2009. Importance of mesophyll diffusion conductance in estimation of plant photosynthesis in the field. *Journal of Experimental Botany* **60**: 2271–2282.

Niinemets Ü, Ellsworth DS, Lukjanova A, Tobias M. 2001. Site fertility and the morphological and photosynthetic acclimation of *Pinus sylvestris* needles to light. *Tree Physiology* **21**: 1231–1244.

Niinemets Ü, Keenan TF, Hallik L. 2015. A worldwide analysis of within-canopy variations in leaf structural, chemical and physiological traits across plant functional types. *New Phytologist* **205**: 973–993.

Niinemets Ü, Tenhunen J. 1997. A model separating leaf structural and physiological effects on carbon gain along light gradients for the shade-tolerant species *Acer saccharum*. *Plant, Cell & Environment* **20**: 845–866.

Ordonez A, Olff H. 2013. Do alien plant species profit more from high resource supply than natives? A trait-based analysis. *Global Ecology and Biogeography* **22**: 648–658.

Patrick LD, Ogle K, Tissue DT. 2009. A hierarchical Bayesian approach for estimation of photosynthetic parameters of C_3 plants. *Plant, Cell & Environment* **32**: 1695–1709.

Piao S, Sitch S, Ciais P, Friedlingstein P, Peylin P, Wang X, Ahlström A, Anav A, Canadell JG, Cong N et al. 2013. Evaluation of terrestrial carbon cycle models for their response to climate variability and to CO_2 trends. *Global Change Biology* **19**: 2117–2132.

Prentice IC, Dong N, Gleason SM, Maire V, Wright IJ. 2014. Balancing the costs of carbon gain and water transport: testing a new theoretical framework for plant functional ecology. *Ecology Letters* **17**: 82–91.

Prentice IC, Farquhar G, Fasham M, Goulden ML, Heimann M, Jaramillo V, Kheshgi H, LeQuéré C, Scholes RJ, Wallace DW. 2001. The carbon cycle and atmospheric carbon dioxide. In: Houghton JT, Ding Y, Griggs DJ, Noguer M, van der Linden PJ, Dai X, Maskell K, Johnson CA, eds. *Climate Change 2001: the scientific basis. Contributions of Working Group I to the third assessment report of the Intergovernmental Panel on Climate Change*. Cambridge, UK: Cambridge University Press, 185–237.

Reich PB, Oleksyn J, Wright IJ. 2009. Leaf phosphorus influences the photosynthesis–nitrogen relation: a cross-biome analysis of 314 species. *Oecologia* **160**: 207–212.

Reich PB, Luo Y, Bradford JB, Poorter H, Perry CH, Oleksyn J. 2014. Temperature drives global patterns in forest biomass distribution in leaves, stems, and roots. *Proceedings of the National Academy of Sciences, USA* **111**: 13721–13726.

Reich PB, Walters MB, Ellsworth DS. 1997. From tropics to tundra: global convergence in plant functioning. *Proceedings of the National Academy of Sciences, USA* **94**: 13730–13734.

Reu B, Zaehle S, Proulx R, Bohn K, Kleidon A, Pavlick R, Schmidtlein S. 2011. The role of plant functional trade-offs for biodiversity changes and biome shifts under scenarios of global climatic change. *Biogeosciences* **8**: 1255–1266.

Rogers A. 2014. The use and misuse of Vc, max in earth system models. *Photosynthesis Research* **119**: 15–29.

Rogers A, Ellsworth DS, Humphries SW. 2001. Possible explanation of the disparity between the *in vitro* and *in vivo* measurements of Rubisco activity: a study in loblolly pine grown in elevated pCO2. *Journal of Experimental Botany* **52**: 1555–1561.

Rogers A, Humphries SW. 2000. A mechanistic evaluation of photosynthetic acclimation at elevated CO_2. *Global Change Biology* **6**: 1005–1011.

Serbin SP, Singh A, Desai AR, Dubois SG, Jablonski AD, Kingdon CC, Kruger EL, Townsend PA. 2015. Remotely estimating photosynthetic capacity, and its response to temperature, in vegetation canopies using imaging spectroscopy. *Remote Sensing of Environment* **167**: 78–87.

Sharkey TD. 1985. Photosynthesis in intact leaves of C_3 plants: physics, physiology and rate limitations. *The Botanical Review* **51**: 53–105.

Sharkey TD, Bernacchi CJ, Farquhar GD, Singsaas EL. 2007. Fitting photosynthetic carbon dioxide response curves for C_3 leaves. *Plant, Cell & Environment* **30**: 1035–1040.

Sun Y, Gu L, Dickinson RE, Pallardy SG, Baker J, Cao Y, DaMatta FM, Dong X, Ellsworth D, Van Goethem D et al. 2014. Asymmetrical effects of mesophyll conductance on fundamental photosynthetic parameters and their relationships estimated from leaf gas exchange measurements. *Plant, Cell & Environment* **37**: 978–994.

Tarvainen L, Wallin G, Räntfors M, Uddling J. 2013. Weak vertical canopy gradients of photosynthetic capacities and stomatal responses in a fertile Norway spruce stand. *Oecologia* 173: 1179–1189.

Tcherkez G, Boex-Fontvieille E, Mahé A, Hodges M. 2012. Respiratory carbon fluxes in leaves. *Current Opinion in Plant Biology* 15: 308–314.

Uddling J, Teclaw RM, Pregitzer KS, Ellsworth DS. 2009. Leaf and canopy conductance in aspen and aspen-birch forests under free-air enrichment of carbon dioxide and ozone. *Tree physiology* 29: 1367–1380.

Verheijen L, Brovkin V, Aerts R, Bönish G, Cornelissen J, Kattge J, Reich P, Wright I, Van Bodegom P. 2013. Impacts of trait variation through observed trait-climate relationships o performance of a representative earth system model: a conceptual analysis. *Biogeosciences* 10: 5497–5515.

Walker AP, Beckerman AP, Gu L, Kattge J, Cernusak LA, Domingues TF, Scales JC, Wohlfahrt G, Wullschleger SD, Woodward FI. 2014. The relationship of leaf photosynthetic traits – V_{cmax} and J_{max} – to leaf nitrogen, leaf phosphorus, and specific leaf area: a meta-analysis and modeling study. *Ecology and Evolution* 4: 3218–3235.

Wang H, Prentice I, Davis T. 2014. Biophysical constraints on gross primary production by the terrestrial biosphere. *Biogeosciences* 11: 5987–6001.

Wang Y, Lu X, Wright I, Dai Y, Rayner P, Reich P. 2012. Correlations among leaf traits provide a significant constraint on the estimate of global gross primary production. *Geophysical Research Letters* 39: L19405.

Way DA, Yamori W. 2014. Thermal acclimation of photosynthesis: on the importance of adjusting our definitions and accounting for thermal acclimation of respiration. *Photosynthesis research* 119: 89–100.

Wilson KB, Baldocchi DD, Hanson PJ. 2000. Spatial and seasonal variability of photosynthetic parameters and their relationship to leaf nitrogen in a deciduous forest. *Tree Physiology* 20: 565–578.

Wright IJ, Reich PB, Cornelissen JH, Falster DS, Groom PK, Hikosaka K, Lee W, Lusk CH, Niinemets Ü, Oleksyn J *et al.* 2005. Modulation of leaf economic traits and trait relationships by climate. *Global Ecology and Biogeography* 14: 411–421.

Wright SJ, Kitajima K, Kraft NJ, Reich PB, Wright IJ, Bunker DE, Condit R, Dalling JW, Davies SJ, Díaz S *et al.* 2010. Functional traits and the growth-mortality trade-off in tropical trees. *Ecology* 91: 3664–3674.

Wullschleger SD. 1993. Biochemical limitations to carbon assimilation in C3 plants – a retrospective analysis of the A-Ci curves from 109 species. *Journal of Experimental Botany* 44: 907.

Xu C, Fisher R, Wullschleger SD, Wilson CJ, Cai M, McDowell NG. 2012. Toward a mechanistic modeling of nitrogen limitation on vegetation dynamics. *PLoS ONE* 7: e37914.

Ziehn T, Knorr W, Scholze M. 2011. Investigating spatial differentiation of model parameters in a carbon cycle data assimilation system. *Global Biogeochemical Cycles* 25: GB2021.

Supporting Information

Additional supporting information may be found in the online version of this article.

Fig. S1 Climatic space covered by this study shown by density hexagons.

Fig. S2 Residuals ($V_{cmax} - \hat{V}_{cmax}$) shown as a function of a moisture index and elevation.

Fig. S3 Residuals ($V_{cmax} - \hat{V}_{cmax}$) shown as a function of the number of annual growing degree-days > 0 and > 5°C.

Fig. S4 Fitted $R_{day} : V_{cmax}$ ratio and R_{day} as a function of leaf temperature using the Badger & Collatz (1977) parameters.

Fig. S5 Fitted $R_{day} : V_{cmax}$ ratio and R_{day} as a function of leaf temperature using the Crous *et al.* (2013) parameters.

Please note: Wiley Blackwell are not responsible for the content or functionality of any supporting information supplied by the authors. Any queries (other than missing material) should be directed to the *New Phytologist* Central Office.